



1 **SWAT Modeling of Water Quantity and Quality in the Tennessee River Basin:**
2 **Spatiotemporal Calibration and Validation**

3 Gangsheng Wang^{1,2,*}, Henriette I. Jager^{1,2}, Latha M. Baskaran¹, Tyler F. Baker³, Craig C.
4 Brandt⁴

5

6 ¹Environmental Sciences Division, Oak Ridge National Laboratory, Oak Ridge, TN 37831 USA

7 ²Climate Change Science Institute, Oak Ridge National Laboratory, Oak Ridge, TN 37831 USA

8 ³Tennessee Valley Authority, Knoxville, TN 37902 USA

9 ⁴Biosciences Division, Oak Ridge National Laboratory, Oak Ridge, TN 37831 USA

10

11 *Corresponding Author: **Gangsheng Wang**

12 Bldg 4500N, Room F129S, MS-6301

13 Oak Ridge National Laboratory

14 Oak Ridge, TN 37831-6301

15 wangg@ornl.gov

16

17 Notice: This manuscript has been authored by UT-Battelle, LLC under Contract No. DE-AC05-

18 00OR22725 with the US Department of Energy. The United States Government retains and the

19 publisher, by accepting the article for publication, acknowledges that the United States

20 Government retains a non-exclusive, paid-up, irrevocable, world-wide license to publish or

21 reproduce the published form of this manuscript, or allow others to do so, for United States

22 Government purposes. The Department of Energy will provide public access to these results of

23 federally sponsored research in accordance with the DOE Public Access Plan

24 (<http://energy.gov/downloads/doe-public-access-plan>).



25 **Abstract**

26 Model-data comparisons are always challenging, especially when working at a large spatial
27 scale and evaluating multiple response variables. We implemented the Soil and Water
28 Assessment Tool (SWAT) to simulate water quantity and quality for the Tennessee River Basin.
29 We developed three innovations to overcome hurdles associated with limited data for model
30 evaluation: 1) we implemented an auto-calibration approach to allow simultaneous calibration
31 against multiple responses, including intermediate response variables, 2) we identified empirical
32 spatiotemporal datasets to use in our comparison, and 3) we compared functional patterns in
33 landuse-nutrient relationships between SWAT and empirical data. Comparing monthly SWAT-
34 simulated runoff against USGS data produced satisfactory median Nash-Sutcliffe Efficiencies of
35 0.83 and 0.72 for calibration and validation periods, respectively. SWAT-simulated water quality
36 responses (sediment, TP, TN, and inorganic N) reproduced the seasonal patterns found in
37 LOADEST data. SWAT-simulated spatial TN loadings were significantly correlated with
38 empirical SPARROW estimates. The spatial correlation analyses indicated that SWAT-modeled
39 runoff was primarily controlled by precipitation; sedimentation was controlled by topography;
40 and NO₃ and soluble P were highly influenced by land management, particularly the proportion
41 of agricultural lands in a subbasin.

42

43 **Keywords:** model calibration, validation, reservoir, runoff, SWAT, Tennessee River, water
44 quality



45 **1 Introduction**

46 The Energy Independence and Security Act (EISA) of 2007 set a target for US production of
47 over 36 billion gallons of renewable fuels annually by 2022 (EISA, 2007). Because agricultural
48 development has historically been associated with impacts on water quality (Dodds and Oakes,
49 2008), converting the lands needed to meet EISA targets heightened concerns for the nation's
50 rivers and lakes, as well as for downstream estuaries. The health of waters in the Tennessee
51 River Basin (TRB) is of particular interest because this region supports one of the most
52 biologically diverse river fauna in North America (Haag and Williams, 2014; Keck et al., 2014).
53 Previous studies have shown higher nutrient and sediment loadings in non-forested, human
54 influenced watersheds in the TRB (Scott et al., 2002). Evaluating changes in water quality
55 associated with large-scale regional shifts in land-use and management requires process-based
56 modeling of hydrology and nutrient dynamics (Wellen et al., 2015). Process-based models are
57 favored whenever projections beyond historical conditions are needed because these models
58 incorporate the processes leading to change and do not require extrapolation of statistical
59 relationships beyond the range represented in the data.

60 Process-oriented models like the Soil & Water Assessment Tool (SWAT) (Arnold and Fohrer,
61 2005; Srinivasan et al., 1998) incorporate current understanding of linkages between watershed
62 properties and water quality responses, but they are also difficult to calibrate (Wang and Chen,
63 2012). Although evaluation of multiple responses simulated by spatially-distributed process-
64 based models over time and space is strongly encouraged (Cao et al., 2006; Wellen et al., 2015),
65 such comprehensive evaluations are limited by the availability of spatial and long-term temporal
66 data. This challenge is compounded for models applied at a regional scale because monitoring
67 efforts tend to be local in scale and of short duration, especially for water quality (Hoos and



68 McMahon, 2009). As such, we see a role for empirical models in the calibration and validation
69 of regional-scale models.

70 Empirical models have previously been fitted to spatial and temporal nutrient loads in the US
71 (Saad et al., 2011). The monthly instream nutrient fluxes were estimated using LOADEST
72 (LOAD ESTimator) developed by the United States Geological Survey (USGS) (Runkel et al.,
73 2004; USGS, 2015). LOADEST assists in developing regression models for estimating nutrient
74 loads or fluxes over a user-defined time interval based on functions of streamflow, time, and
75 additional user-specified variables (Runkel et al., 2004). The SPARROW (SPATIally Reference
76 Regressions On Watershed attributes) is also a model developed by USGS that relates water
77 quality measurements to characteristics of watersheds (Hoos and McMahon, 2009; Saad et al.,
78 2011) to estimate nutrient loads/fluxes. Both models represent empirical relationships most
79 important during the historical period and smooth out the noise inherent in fine-resolution
80 temporal water-quality measurements.

81 When seeking regional surveys suitable for calibration, data may not be available for exactly
82 the outputs produced by the model. However, flexibility in assimilating data can be achieved by
83 comparing against intermediate or synthetic response variables. Several SWAT calibration tools
84 are available, e.g., SWAT-CUP 2012 (Abbaspour, 2014), the Auto-Calibration tool (Van
85 Griensven, 2005), and the R-SWAT-FME framework (Wu and Liu, 2014); however, these tools
86 do not include intermediate or synthetic response variables to compare against. This limitation
87 prevented us from calibrating SWAT using the final water quantity and quality responses if the
88 corresponding observations (or datasets) were not available.

89 This paper presents solutions to the aforementioned challenges, including fitting regional-
90 scale SWAT model when there is limited spatial and long-term water quality data available and



91 representation of reservoirs in a highly regulated watershed. We describe efforts to implement
92 SWAT modeling of water quantity and quality for the TRB including the configuration of 22
93 reservoirs. We incorporate the Shuffled Complex Evolution algorithm (Duan et al., 1992) into
94 SWAT2012 to enable auto-calibration of the model against multiple hydrologic (i.e., water
95 quantity) and water quality response variables (including intermediate and synthetic response
96 variables) at multiple sites. We calibrate and validate SWAT water quantity and quality against
97 empirically modeled datasets available from the USGS throughout the conterminous US. We
98 also used functional validation to compare primary drivers controlling runoff and water quality
99 in the process-based SWAT model and the empirical models. Functional validation goes beyond
100 adding a stamp of approval (i.e., validation), instead comparing relationships to understand
101 differences and guide future modeling or data collection efforts. The approach described here can
102 be applied in other regions of the US where the required empirical models have been developed.

103

104 **2 Materials and Methods**

105 **2.1 Study Area**

106 The Tennessee River Basin (TRB), a tributary basin of the Mississippi River Basin, is located
107 in the southeastern part of the United States (USGS, 2014b) (Fig. 1). There are significant
108 physiographic differences in the eastern and western portions of the basin (Price and Leigh,
109 2006). Forest cover is the dominant natural vegetation in the basin. In the western portion,
110 alluvial plains produced rich soils. The middle of the basin, which was historically covered by
111 bottomland forest and prairie, now supports high percentages of pasture and cropland. Eastward,
112 the geology becomes more mountainous and dominated by limestone with sandstone ridges. The
113 easternmost portion of the basin lies in the rugged Blue Ridge and Southern Appalachian



114 provinces with relatively poor soils (Price and Leigh, 2006). The TRB area has a subtropical
115 climate (warm, humid summers, mild winters) (Sagona, 2003). December through early May is
116 the major flood season (TVA, 2014). Since the 1930's, the TRB has been impounded by a series
117 of dams (reservoirs), most of which are managed by the Tennessee Valley Authority (TVA).
118 Main-stem Tennessee River dams are operated in “run-of-river” mode to support river navigation
119 and generate hydroelectric power. Dams on the tributaries function as storage impoundments and
120 are used primarily for flood control (TVA, 2014). Kentucky Dam is 35 km (22 mi) upstream
121 from Paducah, Kentucky, where the Tennessee River flows northwest into the Ohio River (Fig.
122 1).

123 **2.2 Watershed Delineation and Definition of SWAT Hydrologic Response Units**

124 SWAT (Version 2012/Revision 627) was used to model water quantity and water quality
125 (Arnold et al., 2012). The Digital Elevation Model (DEM) data (1-arc-second, c.a. 30 m) for
126 TRB was downloaded from the National Elevation Dataset
127 (<http://nationalmap.gov/elevation.html>). We conducted watershed delineation in ArcSWAT
128 (Winchell et al., 2013) based on (i) USGS-defined 8-digit Hydrologic Unit Codes (Jager et al.,
129 2015) (HUC8, Fig. 1), and (ii) major stream gages and reservoirs (Fig. 1). Watershed delineation
130 of the TRB using the DEM resulted in a drainage area of 106,124 km². Twenty-two (22)
131 reservoirs were included in the SWAT setup (Fig. 1). SWAT includes a reservoir module that
132 can represent these waterbodies in the watershed (Chen et al., 2015; Wang and Xia, 2010). The
133 reservoir outflow may be calculated by one of the four methods provided by SWAT (Arnold et
134 al., 2012): (i) average annual release rate for uncontrolled reservoir; (ii) measured monthly
135 outflow; (iii) simulated controlled outflow with target release; and (iv) measured daily outflow.



136 The last method (i.e., IRESCO = 3, measured daily outflow) was adopted in this study and TVA
137 provided daily reservoir outflow rates from 1985 to 2013.

138 Hydrological Response Units (HRUs) represent unique combinations of soil type, slope, and
139 land use or land cover. STATSGO soil map units (Soil Survey Staff, 1994) that comprised more
140 than 10% of a subbasin were retained. We discretized slope into four categories: <1%, 1–2%, 2–
141 5%, and >5%. We used the 2009 Cropland Data Layer (CDL-2009) (USDA-NASS, 2014) to
142 represent land use/land cover (Jager et al., 2015). Natural vegetation in TRB is dominated by
143 forest (59.4%) and grassland (11.7%). The major crops in TRB are hay (non-Alfalfa, 9.7%),
144 soybeans (1.7%), and corn (1.5%). We retained land-use classes that comprised more than 2%
145 area of a subbasin. This protocol created a total of 4,026 distinct HRUs in 55 subbasins.

146 **2.3 Meteorological Forcings**

147 We downloaded historical meteorological observation from DAYMET (Thornton et al., 1997)
148 estimated for the center of each HUC8 (Fig. 1) over the period 1980–2014 (35 years). Daily
149 meteorological variables include total precipitation (mm), maximum and minimum temperatures
150 (°C), and solar radiation ($\text{MJ m}^{-2} \text{d}^{-1}$). Two additional variables (wind speed and relative
151 humidity) were estimated by the SWAT model's climate generator (Gassman et al., 2007). The
152 mean annual precipitation (MAP) on HUC8 units ranged from 1129 to 1715 mm with an average
153 of 1433 mm during 1980-2014.

154 **2.4 Model Calibration**

155 Existing auto-calibration routines in the SWAT model are not designed to calibrate against
156 intermediate response variables (e.g., HUC8 runoff and NO_3+NO_2). For this effort, we
157 incorporated the Shuffled Complex Evolution (SCE) algorithm (Duan et al., 1992) into the
158 source code of SWAT2012 model to implement auto-calibration (Fig. 2). SCE is a stochastic



159 optimization algorithm that has been widely used in calibration of hydrological models including
160 SWAT (Wang and Xia, 2010; Zhang et al., 2009). We calibrated 39 parameters (Table 1)
161 governing the hydrologic (i.e., water quantity) and water quality processes in SWAT. The 39
162 parameters were selected based on the sensitivity analyses in previous studies (Abbaspour et al.,
163 2007; Baskaran et al., 2010; Bekele and Nicklow, 2007; Santhi et al., 2001; Wang et al., 2014;
164 Wu and Liu, 2012). Generally, these parameters were calibrated step by step. The hydrologic
165 parameters (No. 1–14) were first calibrated against hydrologic response variables (i.e., water
166 quantity variables, e.g., streamflow or runoff). The second step was to calibrate the water quality
167 parameters (No. 15–39) using water quality measurements (e.g., sediment, nitrogen, and/or
168 phosphorus), where a subset of the parameters might be calibrated depending on the response
169 variables as described below.

170 Fifteen types of calibrations with regard to various response variables (See Supplement Table
171 S1) were defined in our current auto-calibration tool. The first five types correspond to five
172 hydrologic response variables: daily streamflow, monthly streamflow, daily reservoir storage,
173 daily soil water content, and monthly runoff on subbasin or HUC8; the next five types include
174 monthly nutrient (sediment, nitrogen, phosphorus) fluxes (metric tons per month); and the last
175 five types refer to instream monthly nutrient concentration (mg/L). Other response variables
176 could also be defined and added to this calibration framework.

177 Criteria used to assess model performance include:

178 (1) Nash-Sutcliffe Efficiency (NSE, Eq. 1):

179

$$NSE = 1 - \frac{\sum_{i=1}^n [Y_{sim}(i) - Y_{obs}(i)]^2}{\sum_{i=1}^n [Y_{obs}(i) - \bar{Y}_{obs}]^2} \quad (1)$$



180 where Y_{obs} and Y_{sim} are the observed and simulated data, respectively; \bar{Y}_{obs} is the mean value of
181 observations; and n and i denote the number of data points and the i th data, respectively. NSE is
182 less than or equal to 1 and may be negative (Moriassi et al., 2007).

183 (2) Percent Bias (PBIAS, Eq. 2):

$$184 \quad PBIAS = \frac{\bar{Y}_{obs} - \bar{Y}_{sim}}{\bar{Y}_{obs}} \times 100\% \quad (2)$$

185 where PBIAS (Moriassi et al., 2007) denotes the deviation of predicted mean value (\bar{Y}_{sim}) from
186 observed mean value (\bar{Y}_{obs}) as a percentage of \bar{Y}_{obs} .

187 According to Moriassi et al. (2007), model simulation is satisfactory if $NSE > 0.5$ and if
188 $|PBIAS| \leq 25\%$ for streamflow (runoff), $|PBIAS| \leq 55\%$ for sediment, and $|PBIAS| \leq 70\%$ for
189 nitrogen (N) and phosphorus (P).

190 The overall objective function is the weighted average of individual objective functions:

$$191 \quad F = \sum_{j=1}^k (w_j \cdot f_j) \quad (3)$$

192 where F denotes the overall objective function of k individual objective functions; f_j is the j th
193 objective function that could be calculated as NSE or $|PBIAS|$ of interested response variable;
194 and w_j is the weighting factor for each f_j .

195 **2.5 Calibration and Validation of Runoff**

196 Because streamflow (discharge) at a station within the TRB is largely a measure of the outflow
197 from the upstream reservoir(s) and because observed reservoir outflow was used in this study,
198 we calibrated hydrologic parameters based on runoff (i.e., total water yield) instead of
199 streamflow. We used the USGS computed monthly runoff (1985–1995) in HUC8(USGS, 2014a)



200 as reference for SWAT calibration, with one year (1985) for model spin-up and 10 years (1986–
 201 1995) for model calibration. Another 18 years (1996–2013) of data were used for model
 202 validation. The USGS HUC8 runoff estimates were generated by combining historical flow data
 203 at USGS stream gages and the corresponding drainage basin boundaries and hydrologic units
 204 boundaries.(USGS, 2014a) In a previous study, this dataset was used to calibrate the Variable
 205 Infiltration Capacity (VIC) model for the conterminous US (Oubeidillah et al., 2014). The
 206 objective of our multi-site calibration of runoff was to calibrate hydrologic parameters (No. 1–14)
 207 of the subbasins within each HUC8. For example, when we implemented calibration in terms of
 208 the HUC8-06010102, the parameters in four subbasins (1, 4, 5 and 6) in this HUC8 were
 209 calibrated. We calculated simulated HUC8 runoff as the area-weighted-average of runoff from
 210 subbasins within each HUC8:

$$211 \quad R_{HUC8} = \sum_{j=1}^m [R_{sub}(j) \times Area_{sub}(j) / Area_{HUC8}] \quad (4)$$

$$212 \quad Area_{HUC8} = \sum_{j=1}^m [Area_{sub}(j)] \quad (5)$$

213 where R_{HUC8} is the runoff in a HUC8; $R_{sub}(j)$ and $Area_{sub}(j)$ are the simulated runoff (mm) and
 214 the area (km²) in the j th subbasin; and $Area_{HUC8}$ is the total area of the HUC8 that includes m
 215 subbasins. The *NSE* of monthly HUC8 runoff was defined as the objective function in hydrologic
 216 calibration.

217 **2.6 Calibration and Validation of Monthly Nutrient Fluxes**

218 Nutrient measurements are sparse in rivers of the TRB. We have attempted to collect in-situ
 219 water quality monitoring data from over 6,000 USGS and EPA (Environmental Protection
 220 Agency) stations within the TRB through the National Water Quality Monitoring Council



221 (NWQMC)'s online Water Quality Portal (WQP) (NWQMC, 2015). However, we did not find
222 long-term water quality data that coincided with our model simulation period (i.e., after 1980's).
223 Therefore, we used the LOADEST (LOAD ESTimator) dataset (Runkel et al., 2004) as reference
224 to calibrate water quality parameters. The LOADEST dataset provided estimates of monthly
225 nutrient fluxes (1996–2006) at the Tennessee River near Paducah, KY (i.e., the outlet of TRB)
226 (USGS, 2015). We used three-year (1994–1996) of data for model spin-up and 10 years (1997–
227 2006) for model calibration. Another seven years (2007–2013) of data were used for model
228 validation. Four water quality variables were available from the LOADEST dataset: sediment,
229 total phosphorus (TP), total nitrogen (TN), and NO_3+NO_2 . The hydrologic parameters (No. 1–14)
230 calibrated against runoff were fixed during the calibration of water quality parameters (No. 15–
231 39). The *NSE* of monthly water quality was defined as the objective function during SWAT
232 calibration. When multiple response variables (e.g., Sediment, TP, TN, NO_3+NO_2) were
233 considered in model calibration, we used Eq. (4) to calculate the overall objective function. In
234 addition, the spatial distribution of mean annual nutrient loadings estimated by the SPARROW
235 model (Hoos and McMahon, 2009) was employed as another dataset for model validation at the
236 HUC8 level. The mean annual loads (MAL) of nutrients at the HUC8 level were calculated as
237 the area-weighted average of the MALs at all subbasins within the HUC8.

238 **2.7 Spatial Correlation Analyses**

239 Understanding how water yield and nutrient loadings vary with watershed characteristics is
240 important for quantifying primary drivers controlling water quantity and quality and for
241 developing nutrient management policies (Hoos and McMahon, 2009). To this end, we
242 implemented spatial correlation analyses between response variables and watershed attributes.
243 For this study, two variables were considered highly correlated if the absolute value of



244 correlation coefficient ($|r|$) was greater than 0.6 and the correlation was significant (p -value <
245 0.05), and moderately correlated if $|r|$ was between 0.2 and 0.6 and the correlation was
246 significant.

247 Based on the 29-year (1985–2013) simulation results from the calibrated SWAT model, we
248 calculated the mean annual values of response variables including Runoff, RC (Runoff
249 Coefficient, i.e., the ratio of runoff to precipitation), Sediment, OrgP (organic phosphorus), SolP
250 (soluble P), MinP (mineral P attached to sediment), TP, TN, OrgN (organic N), and NO_3 . We
251 first conducted spatial correlation analysis between these response variables at the subbasin level.
252 We implemented spatial correlation analysis between the response variables and the subbasin
253 attributes (explanatory variables): Precipitation (mm), Subbasin_Slope (subbasin slope, %),
254 Elevation_Drop (difference between highest and lowest elevations, m), and fractions of major
255 land-use types (Forest_Fraction, Grassland_Fraction, Hay_Fraction, Crop_Fraction,
256 Shrubland_Fraction, Wetlands_Fraction, Water_Fraction, Developed_Fraction, see Supplement
257 Fig. S1).

258 **3 Results and Discussion**

259 In the sections below, we describe calibration and validation of different SWAT model
260 responses including runoff and water quality metrics.

261 **3.1 Runoff**

262 SWAT simulations of TRB runoff were implemented with regard to the period from 1985 to
263 2013. We divided the 29-year runoff dataset into three sub-datasets: (i) a 1-year spin-up period
264 (1985), (ii) a 10-year calibration period (1986–1995), and (iii) an 18-year validation period
265 (1996–2013). The spatial resolution was the 8-digit hydrologic units (HUC8s) throughout the
266 TRB.



267 Hydrologic parameters (No. 1–14 in Table 1) were calibrated by comparing simulated
268 monthly HUC8 runoff with the USGS dataset. As an example, Fig. S2 shows the comparison
269 between the SWAT-simulated monthly runoff (i.e., water yield, denoted by ‘Sim’) and USGS
270 runoff (denoted by ‘Obs’) in HUC8-06040006, which is the outlet HUC8 of TRB. The *NSE*
271 values for this HUC8 were 0.90 and 0.70 for model calibration and validation, respectively.

272 Values of *NSE* across the 32 HUC8s (Fig. 3a) ranged from 0.56 to 0.93 with 50% confidence
273 interval (CI) of 0.74–0.88 (median 0.83); the *PBIAS* values (Fig. 3b) were within a narrow range
274 (–7%–13%). The model also performed well over the validation period, although *NSE* was lower
275 than that during the calibration period, as one would expect. The median *NSE* was 0.72 with 50%
276 CI of 0.57–0.77; and the *PBIAS* values were within the satisfactory range, i.e., $\pm 25\%$, (Moriassi et
277 al., 2007) except for two HUC8s (06010108 and 06010204). Regarding the whole dataset for the
278 combined calibration and validation periods (1986–2013), the median *NSE* was 0.79 (50% CI:
279 0.69–0.84) and all of the *PBIAS* values were within $\pm 25\%$ except for one HUC8 with a
280 marginally satisfactory *PBIAS* (–26%).

281 The SWAT-simulated mean annual runoff (MAR) in the two aforementioned HUC8s
282 (06010108 and 06010204) might be more reasonable than the USGS-estimated MAR. We
283 analyzed the mean annual precipitation (MAP) and MAR data from 1986–2013 and found that
284 the runoff in these two HUC8s might be underestimated in the USGS dataset to some degree
285 (See Fig. S3).

286 3.2 Water Quality

287 The SWAT simulation of water quality began with the year 1996 owing to data availability. The
288 20-year (1994–2013) water quality dataset was also divided into three sub-datasets: (i) a 3-year



289 spin-up period (1994–1996), (ii) a 10-year calibration period (1997–2006), and (iii) a 7-year
290 validation period (2007–2013).

291 The water quality parameters (No. 15–39 in Table 1) were calibrated against the LOADEST
292 dataset by taking into account multiple objectives, i.e., four response variables, including
293 sediment, TP, TN, and NO_3+NO_2 . Calibration greatly improved the performance of the model,
294 particularly for sediment ($NSE = -100$ and 0.06 for pre- and post-calibration, respectively), TP
295 ($NSE = -2.5$ and 0.44 for pre- and post-calibration, respectively), and TN ($NSE = 0.02$ and 0.38
296 for pre- and post-calibration, respectively) (See Supplement Table S2). The NSE values for
297 model validation were not as good as the NSE for calibration, but the $PBIAS$ values (Table S2)
298 were satisfactory except for NO_3+NO_2 (-157%). The squared correlation coefficients (r^2) for TN
299 and TP during both calibration and validation periods equaled or exceeded 0.4 whereas the r^2
300 values for sediment and inorganic N were less than 0.4 (Table S2). SWAT-simulated water
301 quality responses reproduced the seasonal patterns found in LOADEST data during both
302 calibration and validation periods (See Fig. S4).

303 We further conducted the water quality simulation for a longer period of time (1985–2013)
304 than the period for model calibration and calibration (1997–2013). The spatial distributions of
305 SWAT-simulated MALs (1986–2013) of TN and TP were comparable to the SPARROW
306 estimates. The spatial patterns of SWAT-simulated TN and TP at the subbasin level are shown in
307 Fig. 4 and other variables (runoff, RC, sediment, and NO_3) are shown in Fig. S5. The spatial
308 MALs of TN and TP from SWAT were compared with the SPARROW dataset (MALs from
309 1975–2004) at the HUC8 level (Fig. 5). The $PBIAS$ values (between SWAT and SPARROW) for
310 TN (Fig. 5a) at 26 out of 32 HUC8 units were within the range of $\pm 70\%$, and the $PBIAS$ values at
311 three HUC8 were higher than 80% . The 50% CIs of MAL of TN were 2.5 – 6.7 kg N/ha and 4.7 –



312 7.4 kg N/ha by SWAT and SPARROW, respectively. The SWAT-simulated MAL of TN across
313 the 32 HUC8 units was 5.5 kg N/ha, which was 12% lower than the TN loading (6.2 kg N/ha)
314 estimated by SPARROW.

315 As for phosphorus (Fig. 5b), the SWAT-simulated MAL of OrgP+SolP (organic P + soluble
316 P) was 48% lower than the SPARROW-modeled TP, while the SWAT-simulated MAL of TP
317 (organic P + soluble P + mineral P) was 50% higher than the SPARROW-modeled TP. This was
318 because mineral P contributed most (75.2%) to the TP yield and organic P contributed least
319 (8.5%) to TP. The SWAT-simulated MAL of OrgP+MinP (organic P + mineral P, 0.93 kg P/ha)
320 was comparable to the SPARROW-estimated TP (0.88 kg P/ha).

321 The spatial patterns of TN from the two models (SWAT and SPARROW) were significantly
322 correlated with each other ($r = 0.54$, p -value < 0.001). The spatial pattern of SPARROW-
323 estimated TP was not significantly correlated with SWAT-simulated TP, but moderately
324 correlated with SWAT-simulated OrgP+SolP ($r = 0.38$, p -value = 0.03) and highly correlated
325 with SWAT-simulated TN ($r = 0.84$, p -value < 0.001).

326 Different from the multi-site hydrologic calibration for each HUC8, water quality was
327 calibrated against data from one site owing to data availability. Notice that this site (Paducah,
328 KY) is located at the outlet of TRB. In addition, 10 out of 25 water quality parameters are basin-
329 wide parameters (Table 1, denoted by 'basins.bsn') that are spatially identical in SWAT.
330 Therefore, current water quality calibration could represent the overall water quality regime in
331 the watershed. In summary, the temporal comparison of water quality simulations between
332 SWAT and LOADEST and the spatial comparison between SWAT and SPARROW showed a
333 correspondence between process-based SWAT modeling results and those from empirically
334 modeled data in the TRB.



335 **3.3 Spatial Correlation between Response Variables**

336 Functional validation seeks to compare key functional relationships found in process-based
337 models with those in data. This approach goes beyond simple ‘validation’ or casting a stamp of
338 approval on a model to understand the reasons for any remaining differences. We found that
339 SWAT-simulated MALs of MinP (mineral P attached to sediment) and TP were highly
340 correlated with sediment, which confirms that sediment plays an important role in watershed
341 phosphorus dynamics (Fig 6a). The TN yield was highly correlated with NO₃. TN loadings were
342 dominated by NO₃, i.e., the fraction of TN that was NO₃ ranged from 37% to 99% with an
343 average of 80%. TP was not correlated with TN, but OrgP (organic P) was moderately correlated
344 with OrgN (organic N) and SolP (soluble P) was moderately correlated with NO₃, which implies
345 similarity between SolP and NO₃ dynamics and similarity between OrgP and OrgN dynamics in
346 SWAT (Neitsch et al., 2011). The SPARROW-estimated spatial patterns of TN and TP were
347 correlated with each other; however, the SWAT-simulated spatial distributions of TN and TP
348 were decoupled because the MinP component (attached to sediment) in SWAT and TN was
349 dominated by inorganic nitrogen. Nutrient (Sediment, P and N) loadings were not significantly
350 correlated with runoff (Fig. 6a), suggesting that nutrient point-source and non-point sources and
351 other physical landscape variables (Hoos and McMahon, 2009) control variation in nutrient
352 loadings simulated by SWAT.

353 **3.4 Correlation between SWAT Response Variables and Subbasin Attributes**

354 The spatial correlation analyses showed that the response variables differed in their controlling
355 factors. Runoff was highly correlated with precipitation ($r = 0.68$) and moderately and positively
356 related to Forest_Fraction ($r = 0.36$). The runoff coefficient (RC) was moderately and positively
357 correlated with Elevation_Drop ($r = 0.32$) and Subbasin_Slope ($r = 0.31$) (Fig. 6b).



358 Sediment loadings were moderately and positively correlated with Elevation_Drop ($r = 0.47$),
359 which verifies that the representation of topography and topology in this mountainous region
360 drives sediment dynamics (Wellen et al., 2015). We did not find any significant correlation
361 between TP and the aforementioned subbasin attributes. However, OrgP (organic P) was highly
362 associated with Developed_Fraction ($r = 0.64$) that represented human activities in urban area
363 (Hoos and McMahon, 2009); SolP (soluble P) was moderately correlated with Hay_Fraction ($r =$
364 0.43) indicating the influence of agricultural fertilization; and MinP (mineral P) was moderately
365 correlated with Elevation_Drop ($r = 0.37$) that was the primary driver for sediment generation.

366 Organic N (OrgN) was moderately correlated with Wetlands_Fraction ($r = 0.27$) and
367 Shrubland_Fraction ($r = -0.30$). NO_3 was highly correlated with Hay_Fraction ($r = 0.63$) and
368 moderately correlated with Crop_Fraction ($r = 0.48$), mostly owing to the response of NO_3 yield
369 to agricultural fertilization. In addition, NO_3 showed a moderate negative correlation with
370 Forest_Fraction ($r = -0.54$), Subbasin_Slope ($r = -0.44$), and Elevation_Drop ($r = -0.34$). Note
371 that TRB subbasins with steeper slopes generally had more forest and less cropland. The primary
372 drivers controlling TN were the same as those for NO_3 as TN was dominated by NO_3 .

373 **4 Summary**

374 Model-data comparisons are always challenging, especially when working at a large spatial
375 scale and evaluating multiple response variables. We developed three innovations to overcome
376 hurdles associated with limited data for model testing: 1) we implemented an auto-calibration
377 approach to allow simultaneous calibration against multiple responses, including intermediate
378 response variables, 2) we identified empirical modeled datasets interpolated in space and time to
379 use in our comparison, and 3) we compared functional patterns in landuse-nutrient relationships
380 between SWAT and empirical data. Using these innovations, we were able to successfully



381 implement a calibrated model for the river basin and to evaluate performance. The SWAT
382 calibration tool developed in this study can be accessed upon request via GitHub
383 (<https://github.com/wanggangsheng/SWATopt.git>).

384 In addition to quantitative performance evaluation, we also discerned what the most
385 important influences on SWAT responses were. Runoff was mainly controlled by precipitation;
386 runoff coefficient and sedimentation were controlled by topographic attributes; whereas NO₃ and
387 soluble P were highly influenced by land use types, particularly the croplands (hay and other
388 crops). This is likely because our management of these croplands included applying fertilizers
389 containing N and P. Patterns in phosphorus dynamics differed more between the empirical and
390 process-based model than patterns in nitrogen dynamics, suggesting an area for future
391 exploration.

392

393 **AUTHOR INFORMATION**

394 **Corresponding Author**

395 *Tel: +1 (865)576-6685. E-mail: wangg@ornl.gov.

396 **Notes**

397 The authors declare no competing financial interest.

398

399 **Acknowledgements**

400 This material is based upon work supported by the U.S. Department of Energy, Office of Energy
401 Efficiency & Renewable Energy's Bioenergy Technology Program. Oak Ridge National
402 Laboratory is managed by UT-Battelle, LLC for the U.S. Department of Energy under Contract
403 No. DE-AC05-00OR22725. We thank Michelle Thornton for providing DAYMET data and



404 David Gorelick and Jasmine Kreig for discussion on this study. In addition, we appreciate the
405 insightful reviews of Drs. Shih-Chieh Kao and Sujithkumar Surendran Nair.

406

407



420 **References**

- 421 Abbaspour, K. C.: SWAT-CUP 2012: SWAT Calibration and Uncertainty Programs - A User
422 Manual, Swiss Federal Institute of Aquatic Science and Technology (Eawag) Duebendorf,
423 Switzerland, 2014.
- 424 Abbaspour, K. C., Yang, J., Maximov, I., Siber, R., Bogner, K., Mieleitner, J., Zobrist, J., and
425 Srinivasan, R.: Modelling hydrology and water quality in the pre-alpine/alpine Thur
426 watershed using SWAT, *Journal of Hydrology*, 333, 413-430, 2007.
- 427 Arnold, J. G. and Fohrer, N.: SWAT2000: current capabilities and research opportunities in
428 applied watershed modelling, *Hydrological Processes*, 19, 563-572, 2005.
- 429 Arnold, J. G., Kiniry, J. R., Srinivasan, R., Williams, J. R., Haney, E. B., and Neitsch, S. L.: Soil
430 and Water Assessment Tool Input/Output Documentation Version 2012, Texas Water
431 Resources Institute, College Station, TXTR-439, 650 pp., 2012.
- 432 Baskaran, L., Jager, H., Schweizer, P. E., Srinivasan, R., Douglas-Mankin, K., and Arnold, J.:
433 Progress toward evaluating the sustainability of switchgrass as a bioenergy crop using the
434 SWAT model, *Transactions of the Asabe*, 53, 1547-1556, 2010.
- 435 Bekele, E. G. and Nicklow, J. W.: Multi-objective automatic calibration of SWAT using NSGA-
436 II, *Journal of Hydrology*, 341, 165-176, 2007.
- 437 Cao, W. Z., Bowden, W. B., Davie, T., and Fenemor, A.: Multi-variable and multi-site
438 calibration and validation of SWAT in a large mountainous catchment with high spatial
439 variability, *Hydrological Processes*, 20, 1057-1073, 2006.
- 440 Chen, Y., Ale, S., Rajan, N., Morgan, C. L. S., and Park, J.: Hydrological responses of land use
441 change from cotton (*Gossypium hirsutum* L.) to cellulosic bioenergy crops in the



- 442 Southern High Plains of Texas, USA, GCB Bioenergy, doi: 10.1111/gcbb.12304, 2015.
443 n/a-n/a, 2015.
- 444 Dodds, W. K. and Oakes, R. M.: Headwater influences on downstream water quality,
445 Environmental Management, 41, 367-377, 2008.
- 446 Duan, Q. Y., Sorooshian, S., and Gupta, V.: Effective and efficient global optimization for
447 conceptual rainfall-runoff models, Water Resources Research, 28, 1015-1031, 1992.
- 448 EISA: Energy Independence and Security Act of 2007. 110-140, 2007.
- 449 Gassman, P. W., Reyes, M. R., Green, C. H., and Arnold, J. G.: The soil and water assessment
450 tool: Historical development, applications, and future research directions, Transactions of
451 the ASABE, 50, 1211-1250, 2007.
- 452 Haag, W. R. and Williams, J. D.: Biodiversity on the brink: an assessment of conservation
453 strategies for North American freshwater mussels, Hydrobiologia, 735, 45-60, 2014.
- 454 Hoos, A. B. and McMahon, G.: Spatial analysis of instream nitrogen loads and factors
455 controlling nitrogen delivery to streams in the southeastern United States using spatially
456 referenced regression on watershed attributes (SPARROW) and regional classification
457 frameworks, Hydrological Processes, 23, 2275-2294, 2009.
- 458 Jager, H. I., Baskaran, L. M., Schweizer, P. E., Turhollow, A. F., Brandt, C. C., and Srinivasan,
459 R.: Forecasting changes in water quality in rivers associated with growing biofuels in the
460 Arkansas-White-Red river drainage, USA, Global Change Biology: Bioenergy, 7, 774-
461 784, 2015.
- 462 Keck, B. P., Marion, Z. H., Martin, D. J., Kaufman, J. C., Harden, C. P., Schwartz, J. S., and
463 Strange, R. J.: Fish functional traits correlated with environmental variables in a
464 temperate biodiversity hotspot, PLOS ONE, 9, e93237, 2014.



- 465 Moriasi, D., Arnold, J., Van Liew, M., Bingner, R., Harmel, R., and Veith, T.: Model evaluation
466 guidelines for systematic quantification of accuracy in watershed simulations,
467 Transactions of the Asabe, 50, 885-900, 2007.
- 468 Neitsch, S. L., Arnold, J. G., Kiniry, J. R., and Williams, J. R.: Soil and Water Assessment Tool
469 Theoretical Documentation. Version 2009, Texas Water Resources Institute, Texas A&M
470 University System, College Station, TX, 647 pp., 2011.
- 471 NWQMC: Water Quality Portal. National Water Quality Monitoring Council, 2015.
- 472 Oubeidillah, A. A., Kao, S. C., Ashfaq, M., Naz, B. S., and Tootle, G.: A large-scale, high-
473 resolution hydrological model parameter data set for climate change impact assessment
474 for the conterminous US, Hydrol. Earth Syst. Sci., 18, 67-84, 2014.
- 475 Price, K. and Leigh, D. S.: Morphological and sedimentological responses of streams to human
476 impact in the southern Blue Ridge Mountains, USA, Geomorphology, 78, 142-160, 2006.
- 477 Runkel, R. L., Crawford, C. G., and Cohn, T. A.: Load Estimator (LOADEST): A FORTRAN
478 program for estimating constituent loads in streams and rivers, U.S. Geological Survey,
479 Reston, Virginia 2328-7055, 2004.
- 480 Saad, D. A., Schwarz, G. E., Robertson, D. M., and Booth, N. L.: A Multi-Agency Nutrient
481 Dataset Used to Estimate Loads, Improve Monitoring Design, and Calibrate Regional
482 Nutrient SPARROW Models, Journal of the American Water Resources Association, 47,
483 933-949, 2011.
- 484 Sagona, F. J.: Tennessee River Basin Watershed Management Plan, Tennessee River Clean
485 Water Partnership, Rainsville, AL, 148 pp., 2003.



- 486 Santhi, C., Arnold, J. G., Williams, J. R., Dugas, W. A., Srinivasan, R., and Hauck, L. M.:
487 Validation of the SWAT model on a large river basin with point and nonpoint sources,
488 Journal of the American Water Resources Association, 37, 1169-1188, 2001.
- 489 Scott, M. C., Helfman, G. S., McTammany, M. E., Benfield, E. F., and Bolstad, P. V.: Multiscale
490 influences on physical and chemical stream conditions across Blue Ridge landscapes,
491 Journal of the American Water Resources Association, 38, 1379-1392, 2002.
- 492 Soil Survey Staff: U.S. General Soil Map (STATSGO), Natural Resources Conservation Service,
493 U.S. Department of Agriculture, Washington, D.C. , 1994.
- 494 Srinivasan, R., Arnold, J., and Jones, C.: Hydrologic modelling of the United States with the soil
495 and water assessment tool, International Journal of Water Resources Development, 14,
496 315-325, 1998.
- 497 Thornton, P. E., Running, S. W., and White, M. A.: Generating surfaces of daily meteorological
498 variables over large regions of complex terrain, Journal of Hydrology, 190, 214-251,
499 1997.
- 500 TVA: <http://www.tva.gov>, last access: 8/8/2014 2014.
- 501 USDA-NASS: <http://www.nass.usda.gov/research/Cropland/SARS1a.htm>, last access: 3/16/2014,
502 2014.
- 503 USGS: <http://waterwatch.usgs.gov/index.php?id=romap3>, last access: 10/1/2014 2014.
- 504 USGS: <http://tn.water.usgs.gov/ltcn/tenn.html>, last access: 4/8/2014 2014.
- 505 USGS: Streamflow and Nutrient Flux at Tennessee River at Highway 60 near Paducah,
506 Kentucky. U. S. Geological Survey, 2015.
- 507 Van Griensven, A.: Sensitivity, auto-calibration, uncertainty and model evaluation in
508 SWAT2005, UNESCO-IHE, Delft, Ntherlands, 2005.



- 509 Wang, G., Barber, M. E., Chen, S., and Wu, J. Q.: SWAT modeling with uncertainty and cluster
510 analyses of tillage impacts on hydrological processes, *Stochastic Environmental Research*
511 and *Risk Assessment*, 28, 225-238, 2014.
- 512 Wang, G. and Chen, S.: A review on parameterization and uncertainty in modeling greenhouse
513 gas emissions from soil, *Geoderma*, 170, 206-216, 2012.
- 514 Wang, G. and Xia, J.: Improvement of SWAT2000 modelling to assess the impact of dams and
515 sluices on streamflow in the Huai River basin of China, *Hydrological Processes*, 24,
516 1455-1471, 2010.
- 517 Wellen, C., Kamran-Disfani, A.-R., and Arhonditsis, G. B.: Evaluation of the Current State of
518 Distributed Watershed Nutrient Water Quality Modeling, *Environmental science &*
519 *technology*, 49, 3278-3290, 2015.
- 520 Winchell, M., Srinivasan, R., Di Luzio, M., and Arnold, J. G.: ArcSWAT Interface for
521 SWAT2012 User's Guide, Blackland Research and Extension Center, Temple, TXTR-
522 439, 464 pp., 2013.
- 523 Wu, Y. and Liu, S.: Improvement of the R-SWAT-FME framework to support multiple variables
524 and multi-objective functions, *Science of the Total Environment*, 466, 455-466, 2014.
- 525 Wu, Y. and Liu, S.: Modeling of land use and reservoir effects on nonpoint source pollution in a
526 highly agricultural basin, *Journal of Environmental Monitoring*, 14, 2350-2361, 2012.
- 527 Zhang, X., Srinivasan, R., Zhao, K., and Liew, M. V.: Evaluation of global optimization
528 algorithms for parameter calibration of a computationally intensive hydrologic model,
529 *Hydrological Processes*, 23, 430-441, 2009.
- 530
- 531



Tables

Table 1. Selected SWAT parameters for model calibration

No	Parameter ^d	Description	Default	Min	Max	Input file	Fortran code
1	CN2	Initial SCS curve number II	85	35	98	*.mgt	Readmgt.f
2	ESCO	Soil evaporation compensation factor	0.95	0.01	1	*.hru	Readhru.f
3	EPKO	Plant uptake compensation factor	1	0.01	1	*.hru	Readhru.f
4	OV_N	Manning's n value for overland flow	0.1	0.01	0.6	*.hru	Readhru.f
5	CH_N2	Manning's n value for main channel	0.014	0.01	0.5	*.rte	Readrte.f
6	CH_K2	Channel effective hydraulic conductivity (mm/hr)	0.001	0.001	150	*.rte	Readrte.f
7	ALPHA_BF	Baseflow alpha factor (days)	0.048	0.001	1	*.gw	Readgw.f
8	GW_DELAY	Ground water delay (days)	31	0.0001	500	*.gw	Readgw.f
9	RCHRG_DP	Deep aquifer percolation fraction	0.05	0.0001	1	*.gw	Readgw.f
10	GW_REVAP	Groundwater revap coefficient	0.02	0.02	0.2	*.gw	Readgw.f
11	GW_SPYLD	Specific yield for shallow aquifer (m ³ /m ³)	0.003	0.0001	0.4	*.gw	Readgw.f
12	SOL_AWC	Available water capacity (mm H ₂ O/mm soil)	0.2	0.01	0.4	*.sol	Readsol.f
13	SOL_K	Saturated hydraulic conductivity (mm/h)	10	0.01	100	*.sol	Readsol.f
14	SURLAG	Surface runoff lag coefficient (days)	4	0.5	12	sub.lag	Readhru.f
15	SPCON	Linear re-entrainment parameter	0.0001	0.0001	0.01	basins.bsn	Readbsn.f
16	SPEXP	Exponent re-entrainment parameter	1	1	2	basins.bsn	Readbsn.f
17	PRF	Adjustment factor for sediment routing in the main channel	1	0.001	2	basins.bsn	Readbsn.f
18	ADJ_PKR	Adjustment factor for sediment routing in tributary channels	1	0.5	2	basins.bsn	Readbsn.f
19	CH_COV	Channel cover factor	0.001	0.001	1	*.rte	Readrte.f
20	CH_EROD	Channel erodibility factor	0.001	0.001	1	*.rte	Readrte.f
21	USLE_K	Soil erodability factor	0.28	0.01	0.65	*.sol	readsol.f
22	BIOMIX	Biological mixing coefficient	0.2	0.01	1	*.mgt	Readmgt.f
23	RSDCO	Residue decomposition factor	0.05	0.02	0.1	basins.bsn	Readbsn.f
24	NPERCO	Nitrogen percolation factor	0.2	0.001	1	basins.bsn	Readbsn.f
25	N_UPDIS	N uptake distribution parameter	20	0.001	100	basins.bsn	Readbsn.f
26	NSETLR	N settling rate in reservoir (m/yr), Line 7 & 8	5.5	1	15	*.lwq	Readlwq.f
27	SHALLST_N	Concentration of NO ₃ in groundwater (mg N/L)	0.0001	0.0001	1000	*.gw	Readgw.f
28	ERORGN	Organic N enrichment for sediment	0.001	0.001	5	*.hru	Readhru.f
29	SOL_ORGN	Initial organic N concentration (mg N kg ⁻¹ soil)	0.01	0.01	50	*.chm	Readchm.f
30	SOL_NO3	Initial NO ₃ concentration in the soil layer (mg N kg ⁻¹ soil)	0.01	0.01	50	*.chm	Readchm.f
31	PPERCO	Phosphorus percolation factor (10 m ³ Mg ⁻¹)	10	10	17.5	basins.bsn	Readbsn.f
32	PHOSKD	Phosphorus soil partitioning coefficient (m ³ Mg ⁻¹)	175	100	200	basins.bsn	Readbsn.f
33	PSP	P sorption coefficient	0.4	0.01	0.7	basins.bsn	Readbsn.f
34	PSETLR	P settling rate in reservoir (m/yr), Line 5 & 6	10	2	20	*.lwq	Readlwq.f
35	BC4	Rate const for mineralization of organic P to dissolved P (1/d)	0.35	0.01	0.7	*.swq	Readswq.f
36	RS5	Organic P settling rate (1/d)	0.05	0.001	0.1	*.swq	Readswq.f
37	ERORGP	Organic P enrichment ratio with sediment loading	0.001	0.001	5	*.hru	readhru.f
38	SOL_ORGP	Initial organic P (mg P kg ⁻¹ soil)	0.01	0.01	50	*.chm	Readchm.f
39	SOL_SOLP	Initial soluble P concentration in the soil layer (mg P kg ⁻¹ soil)	5	0.01	50	*.chm	Readchm.f

^dFour groups of parameters: No. 1–14: Water quantity; No. 15–21: Sediment; No. 22–30: Nitrogen; No. 31–39:

Phosphorus.



Figure Captions

Figure 1. Fifty-five subbasins and 22 reservoirs of the Tennessee River Basin (TRB) in the Soil and Water Assessment Tool (SWAT). The mainstem Tennessee River runs from east to west, exiting the basin below Kentucky Dam.

Figure 2. Integrating the Shuffled Complex Evolution (SCE) algorithm into the Soil and Water Assessment Tool (SWAT) permitted calibration against intermediate response variables.

Figure 3. Model calibration of SWAT-modeled runoff by optimizing hydrologic parameters and validation. The distribution shows values for 32 HUC8 units (8-digit Hydrologic Unit Codes). Measures of model performance are (a) Nash-Sutcliffe Efficiency (NSE), (b) Percent Bias (PBIAS).

Figure 4. Spatial distribution of SWAT-simulated mean annual values at 55 subbasins: (a) TN yield (kg N/ha), (b) TP yield (kg P/ha).

Figure 5. Comparison of spatial distribution of TN and TP yield between SWAT simulation and SPARROW dataset at 32 HUC8 units. SWAT metrics: $\text{OrgP_SolP} = \text{OrgP (organic P)} + \text{SolP (soluble P)}$; $\text{OrgP_MinP} = \text{OrgP} + \text{MinP (mineral P attached to sediment)}$; $\text{SolP_MinP} = \text{SolP} + \text{MinP}$; and $\text{TP} = \text{OrgP} + \text{SolP} + \text{MinP}$.

Figure 6. Spatial correlation analysis (a) between response variables (mean values from 1996 to 2013), (b) between response variables and subbasin attributes. Larger circle denotes higher



correlation coefficient and only significant correlations (p -value < 0.05) are shown. Numbers in (a) denote correlation coefficients. Response variables are: sediment yield (kg TSS/ha), organic phosphorus yield (OrgP, kg P/ha), soluble P yield (SolP, kg P/ha), mineral P yield attached to sediment (MinP, kg P/ha), total P yield (TP = OrgP + SolP + MinP, kg P/ha), total nitrogen yield (TN, kg N/ha), organic N yield (OrgN, kg N/ha), nitrate yield (NO₃, kg N/ha), runoff depth (mm), and runoff coefficient (RC, ratio of runoff to precipitation).



Figures

Figure 1

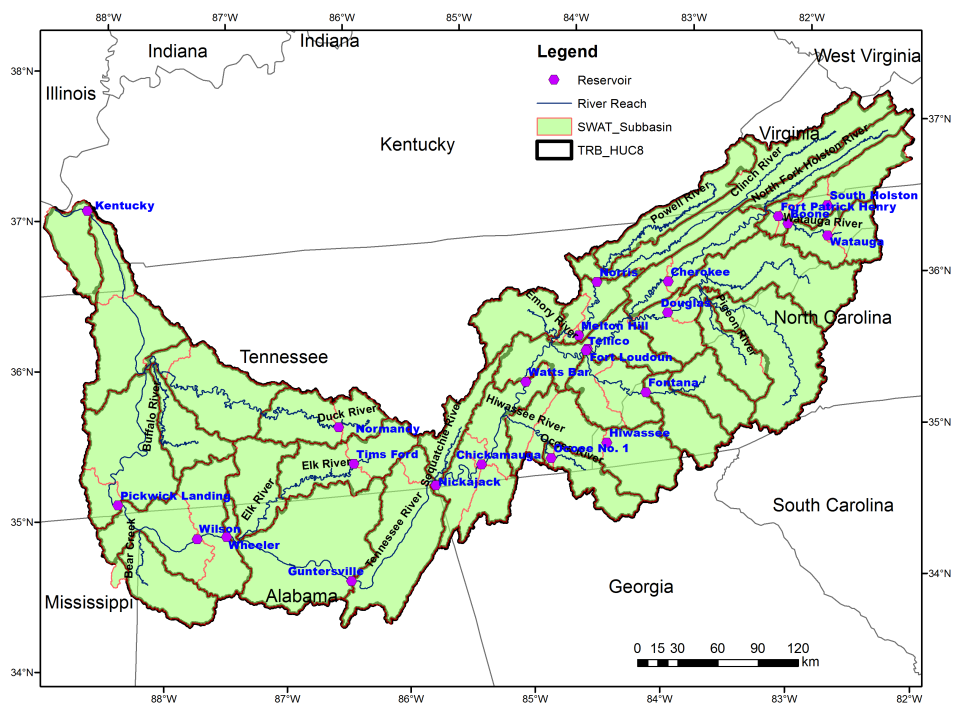




Figure 2

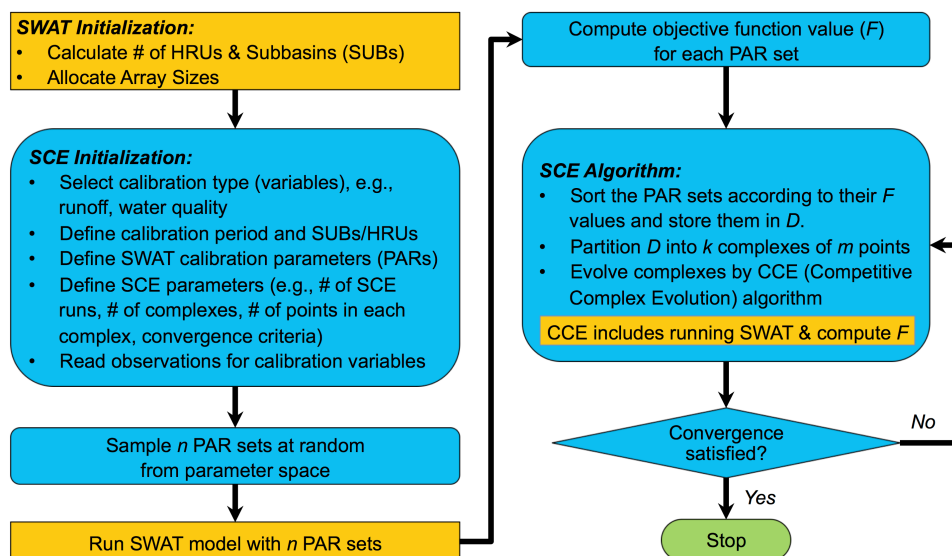




Figure 3

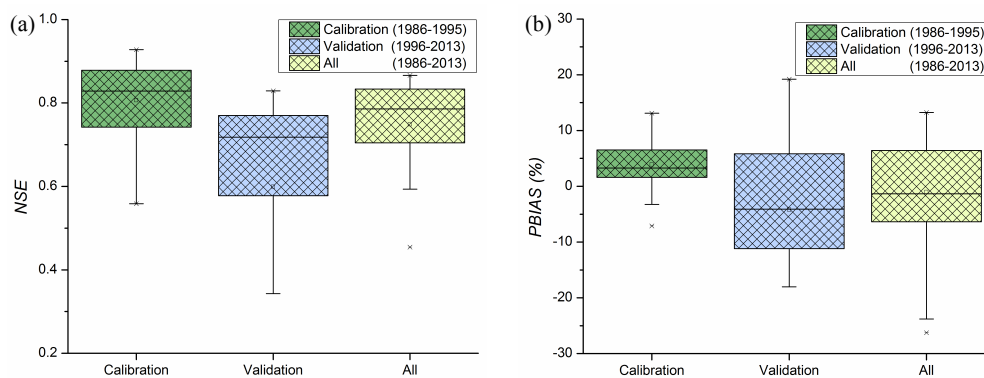




Figure 4

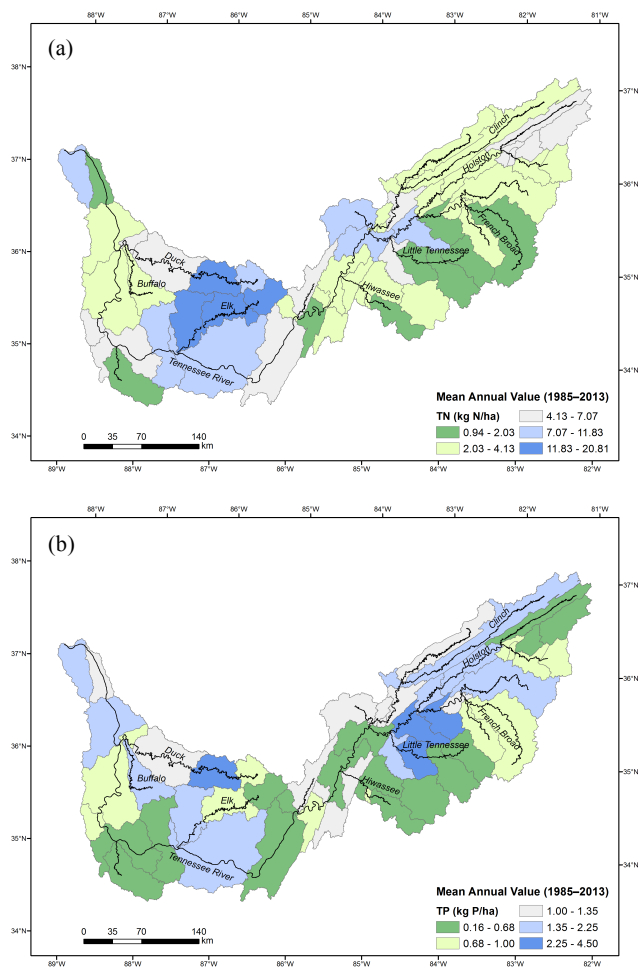




Figure 5

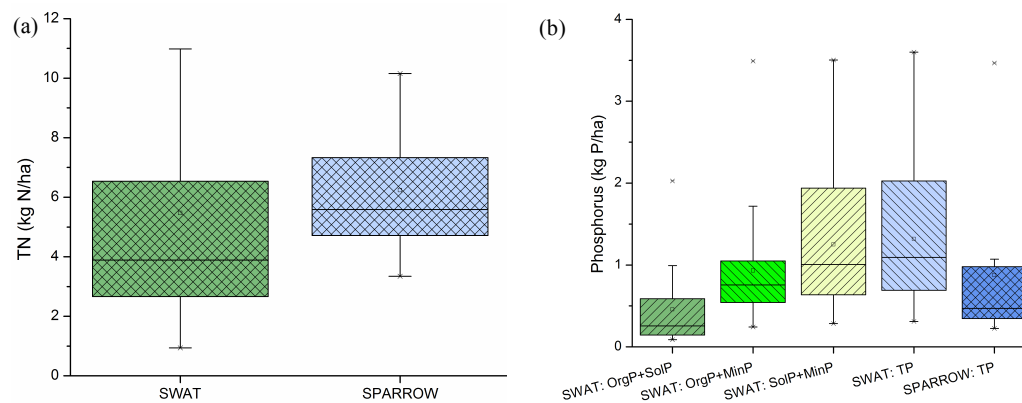




Figure 6

